



GPR83 Engages Endogenous Peptides from Two Distinct Precursors to Elicit Differential Signaling^S

Seshat M. Mack,² Ivone Gomes,² Amanda K. Fakira,¹  Mariana Lemos Duarte, Achla Gupta Lloyd Fricker, and  Lakshmi A. Devi

Department of Pharmacological Sciences, Icahn School of Medicine at Mount Sinai, New York, New York (S.M.M., I.G., A.K.F., M.L.D., A.G., L.A.D.) and Department of Molecular Pharmacology, Albert Einstein College of Medicine, Bronx, New York, New York (L.F.)

Received January 4, 2022; accepted May 3, 2022

ABSTRACT

PEN is an abundant neuropeptide that activates G protein-coupled receptor 83 (GPR83), which is considered a novel therapeutic target due to its roles in regulation of feeding-, reward-, and anxiety-related behaviors. The major form of PEN in the brain is 22 residues in length. Previous studies have identified shorter forms of PEN in mouse brain and neuroendocrine cells; these shorter forms were named PEN18, PEN19, and PEN20, with the number reflecting the length of the peptide. The C-terminal five residues of PEN20 are identical to the C-terminus of a procholecystokinin (proCCK)-derived peptide, named proCCK56–62, that is present in mouse brain. ProCCK56–62 is highly conserved across species, although it has no homology to the bioactive cholecystokinin domain. ProCCK56–62 and a longer form, proCCK56–63, were tested for their ability to engage GPR83. Both peptides bind GPR83 with high affinity, activate second messenger pathways, and induce ligand-mediated receptor endocytosis. Interestingly, the shorter PEN peptides, ProCCK56–62 and ProCCK56–63, differentially activate signal transduction pathways. Whereas PEN22 and PEN20

facilitate receptor coupling to G α i, PEN18, PEN19, and ProCCK peptides facilitate coupling to G α s. Furthermore, the ProCCK peptides exhibit dose-dependent G α subtype selectivity in that they facilitate coupling to G α s at low concentrations and G α i at high concentrations. These data demonstrate that peptides derived from two distinct peptide precursors can differentially activate GPR83 and that GPR83 exhibits G α subtype preference depending on the nature and concentration of the peptide. These results are consistent with the emerging idea that endogenous neuropeptides function as biased ligands.

SIGNIFICANCE STATEMENT

We found that peptides derived from procholecystokinin (proCCK) bind and activate G protein-coupled receptor 83, which is known to bind peptides derived from proSAAS. Different forms of the proCCK- and proSAAS-derived peptides show biased agonism, activating G α s or G α i depending on the length of the peptide and/or its concentration.

Introduction

G protein-coupled receptor 83 (GPR83), first identified in murine thymoma cells as a receptor upregulated after treatment with the glucocorticoid dexamethasone (Harrigan et al., 1989; Harrigan et al., 1991; Wang et al., 2001), was later found to exhibit expression in the brain (Pesini et al., 1998; Brezillon et al., 2001). Studies reported robust GPR83 expression in regions involved in modulation of food intake (Muller et al., 2013b; Lueptow et al., 2018; Mack et al., 2019) and reward behaviors (Pesini et al., 1998; Lueptow et al., 2018;

Fakira et al., 2019). Moreover, GPR83 knockout (KO) mice demonstrate altered food intake and anxiety-related behaviors (E Vollmer et al., 2013; Muller et al., 2013b; Fakira et al., 2021). Recent studies show that knockdown of GPR83 in the ventral striatum attenuates morphine-induced reward (Fakira et al., 2019). Together, this provides support for involvement of GPR83 in the regulation of feeding, stress, and reward behaviors and indicates that it is a potential therapeutic target (Lueptow et al., 2018).

In 2016, the neuropeptide PEN was identified as a potent and selective ligand for GPR83 (Gomes et al., 2016), an observation that has been independently confirmed (Foster et al., 2019; Parobchak et al., 2020). PEN was first identified in 2000 in a search for substrates of carboxypeptidase E (CPE), an important enzyme in the biosynthesis of most peptide hormones and neuropeptides (Fricker et al., 2000). The PEN precursor, named proSAAS, gives rise to several distinct peptides including big and little forms of SAAS, GAV, and LEN. Previous studies have implicated big LEN and PEN in the regulation of feeding (Wardman et al., 2011). Big LEN is a ligand for GPR171, which, like GPR83,

This research was funded by National Institutes of Health grants: National Institute on Drug Abuse [Grant R01-DA008863], National Institute of Neurologic Disorders and Stroke [Grant R01-NS026880], and National Center for Advancing Translational Sciences [Grant 1R03-TR003647-01] (to L.A.D.) and diversity supplement [R01-DA008863S] (to S.M.M.).

The authors do not have any conflicts of interest to disclose.

¹Current affiliation: Department of Biomedical Sciences, Cooper Medical School of Rowan University, Camden, New Jersey.

²S.M.M. and I.G. contributed equally to this work.

dx.doi.org/10.1124/molpharm.122.000487.

^S This article has supplemental material available at molpharm.aspetjournals.org.

ABBREVIATIONS: cat. no., Catalog Number; CCK, cholecystokinin; CPE, carboxypeptidase E; GPCR, G protein-coupled receptor; GPR83, G protein-coupled receptor 83; KO, knockout; mPEN, mouse PEN; PLC, phospholipase C; proCCK, procholecystokinin; WT, wild-type.

has been implicated in feeding and reward behaviors (Gomes et al., 2013; Wardman et al., 2016). Little LEN does not bind to GPR171, illustrating the importance of peptide processing on the resulting biologic activity.

Most studies on PEN focused on the full-length peptide, which is 22 amino acids in length (Fricker et al., 2000; Wardman et al., 2011; Gomes et al., 2016). Smaller forms of PEN lacking 2 or more C-terminal residues were identified in mouse brain and in AtT20 cells overexpressing proSAAS (Mzhavia et al., 2002; Fricker, 2010). These forms were named PEN20, PEN19, and PEN18, with the number indicating the length (Mzhavia et al., 2002) (Fig. 1). Interestingly, PEN20 has a similar C-terminal sequence as a peptide derived from procholecystokinin (proCCK) that has been identified by peptidomic analyses of mouse brain (Fricker, 2010) (Fig. 1). This proCCK peptide corresponds to residues 56-62 of proCCK (numbering from the initiation Met). ProCCK 56-62 and PEN20 have the same five residues on their C-termini: LGALL. Shorter and longer forms of this proCCK peptide were also found in mouse brain. The “LGALL” sequence in proCCK is highly conserved across species, but there are no studies reporting the biologic activity of this peptide. Most of the previous studies on proCCK-derived peptides have focused on the 8-residue cholecystokinin (CCK) peptide, or N-terminally-extended forms CCK-12, CCK-33, and others (Beinfeld, 2003; Goetze and Rehfeld, 2019). CCK plays an important physiologic role in digestion and functions as a neuropeptide in the central nervous system to modulate satiety and suppress hunger (Rehfeld, 2017; Okonkwo et al., 2020).

There are many examples where two or more distinct neuropeptides bind to a common receptor. A classic example is the opioid peptides, with >20 different enkephalin-containing peptides produced from proenkephalin, prodynorphin, and proopio-melanocortin (Fricker et al., 2020). All of these peptides bind to the three opioid receptors (μ , δ , and κ), albeit with different affinities and efficacies. Recently, different opioid peptides were found to produce distinct profiles of second-messenger activation at all three opioid receptors (Gomes et al., 2020). Therefore, the first question addressed in this

study was whether PEN20 and shorter peptides bound to GPR83 and if so, whether their activities differed from those of PEN. The second question was whether the proCCK peptides can bind and activate GPR83. Our finding that GPR83 binds the truncated PEN peptides and also the conserved proCCK-derived peptides suggests that it can integrate signaling from distinct neuropeptides. Furthermore, our finding that these peptides exhibit differences in the type and extent of intracellular signaling serves as a foundation for understanding GPR83 signaling both in normal cell function and in pathologic disease states and for the development of small molecule GPR83 ligands as novel therapeutics for the treatment of anxiety, depression, and addiction.

Materials and Methods

Materials. Mouse PEN (mPEN) was obtained from Phoenix Pharmaceuticals, Inc. (Burlingame, CA). CHO cells were from ATCC (Manassas, VA). F12 media was from Gibco/Thermo Fisher (Waltham, MA). FBS was from Biowest (Riverside, MO). PEN18, PEN19, PEN20, PEN22, CCK56-63, CCK56-62, and DYKK-tagged mouse GPR83 cDNA were from Genscript (Piscataway, NJ). Protease inhibitor cocktail [Catalog Number (cat. no.) P2714], p-nitrophenylphosphorylcholine, were from Sigma-Aldrich (St. Louis, MO). [125 I] (cat. no. NEZ033L001MC) and [35 S]GTP γ S (cat. no. NE-G030H250UC) were from PerkinElmer (Shelton, CT). Pierce Iodination Reagent was from Thermo Scientific (Waltham, MA). GF/B filters were from Brandel, Inc. (Gaithersburg, MD). Forskolin and 3-isobutyl-1-methylxanthine were from Tocris Bioscience (Minneapolis, MN). HitHunter cAMP detection kit was from DiscoverRx (Fremont, CA). Anti-DYKK monoclonal antibodies (cat. No. 14793) were from Cell Signaling Technology (Danvers, MA). Anti-mouse antibody coupled to horseradish peroxidase was from Vector Laboratories (Burlingame, CA). *GPR83* knockout (genotyped by quantitative polymerase chain reaction analysis) and control wild-type (WT) mouse brains were generated as described (Muller et al., 2013b). Calcium 6 Assay Kit was from Molecular Devices (San Jose, CA).

Cell Culture. CHO cells were grown in F12 media containing 10% FBS, 1X penicillin-streptomycin solution at 37°C, and 10% CO $_2$ /O $_2$. Cells stably expressing DYKK-tagged mouse GPR83 (CHO-GPR83)

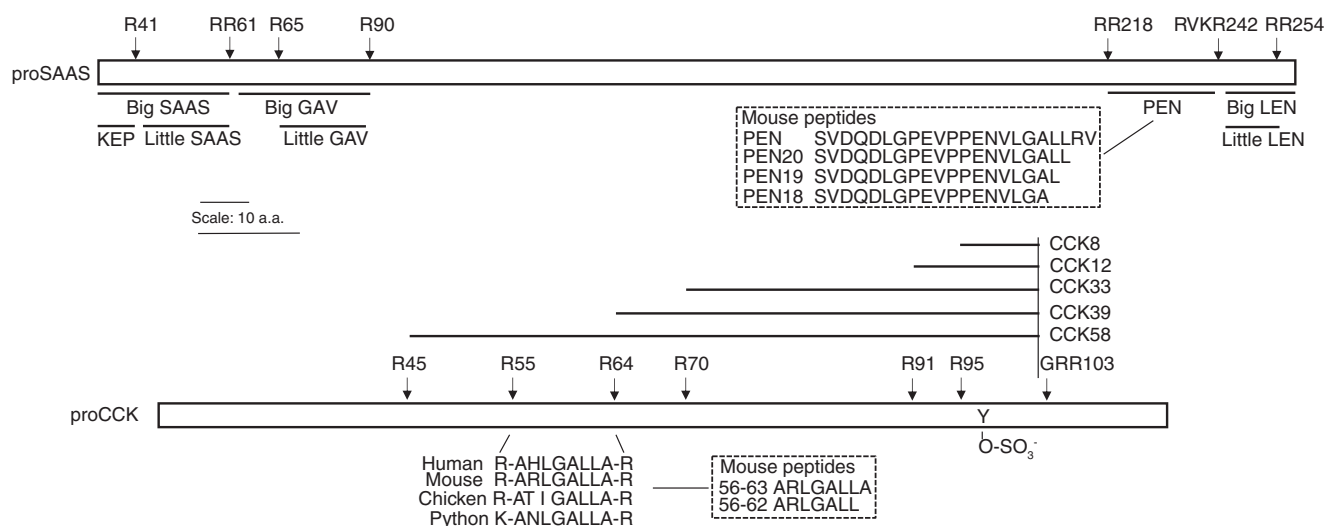


Fig. 1. Schematic representation of peptides generated from the processing of proSAAS and proCCK. Processing of the proSAAS precursor at monobasic and dibasic sites yields Big SAAS, Big GAV, KEP, Little SAAS, Little GAV, PEN, Big LEN, and Little LEN. Mass spectrometric analysis detects the presence of PEN (i.e., PEN22) as well as shorter PEN peptides (PEN18, PEN19, PEN20) (Mzhavia et al., 2002; Fricker, 2010). Processing of proCCK yields CCK8, CCK12, CCK33, CCK39, and CCK58. In addition, mass spectrometric analyses detect the presence of CCK peptides containing the highly conserved LGALL motif that is present in PEN (Mzhavia et al., 2002; Fricker, 2010).

were generated using lipofectamine as per manufacturer's protocol and maintained in growth media containing 500 $\mu\text{g/ml}$ G418. Cells free from mycoplasma contamination were used in our studies. Receptor expression levels were routinely checked by ELISA, binding assays, and quantitative real time-polymerase chain reaction (Gomes et al., 2016). Cells were used up to 6 passages, after which a fresh vial was thawed from liquid nitrogen stocks.

Membrane Preparation. Membranes from CHO and CHO-GPR83 cells and from the striatum of WT or GPR83 knockout (GPR83 KO striatum) mice were prepared as described previously (Gomes et al., 2016). Briefly, cells/striatum were homogenized in 25 volumes (1 g wet weight per 25 ml) of ice-cold 20 mM Tris-Cl buffer containing 250 mM sucrose, 2 mM EGTA, and 1 mM MgCl_2 (pH 7.4), followed by centrifugation at 27,000g for 15 minutes at 4°C. The pellet was resuspended in 25 ml of the same buffer, and the centrifugation step was repeated. The resulting membrane pellet was resuspended in 40 volumes (of original wet weight) of 2 mM Tris-Cl buffer containing 2 mM EGTA and 10% glycerol (pH 7.4). The protein content of the homogenates was determined using the Pierce BCA Protein Assay reagent, after which homogenates were stored in aliquots at -80°C until use.

$[^{125}\text{I}]\text{Tyr-rPEN}$ Displacement Assay

Tyr-rPEN (200 μg) was radioiodinated using $[^{125}\text{I}]$ and Pierce Iodination Reagent as described in the manufacturer's protocol (Thermo Scientific). The specific activity of the iodinated peptide was 53.5 Ci/mmol at the time of iodination (the radiolabeled peptide was used within 60 days of iodination).

Displacement binding assays were carried out for 1 hour at 37°C using 50 mM Tris-Cl (pH 7.4) containing protease inhibitor cocktail; 3 nM of $[^{125}\text{I}]\text{Tyr-rPEN}$; different concentrations (0 to 10 μM) of either PEN18, PEN19, PEN20, PEN22, PEN11-20, PEN11-22, CCK56-63, or CCK56-62; and membranes (20 μg) from either CHO-GPR83 cells, parental CHO cells, or the striatum of wild-type mice. At the end of the incubation period, samples were filtered using a Brandel filtration system and GF/B filters. Filters were washed three times with 3 ml of ice-cold 50 mM Tris-Cl (pH 7.4), and bound radioactivity was measured using a scintillation counter. Membranes from CHO cells alone or GPR83 KO mice striatum were used as controls, showing that $[^{125}\text{I}]\text{Tyr-rPEN}$ did not exhibit binding that could be displaced by PEN22 (Supplemental Fig. 1, A and D).

GTP γ S Assay. $[^{35}\text{S}]\text{GTP}\gamma\text{S}$ binding assays were carried out as described previously (Gomes et al., 2013; Gomes et al., 2016). Briefly, membranes (20 μg) from CHO-GPR83 cells, parental CHO cells, or striatum from wild-type mice were incubated for 1 hour at 30°C with either full-length mPEN (PEN22), PEN18, PEN19, PEN20, PEN11-22, PEN11-20, CCK56-63, or CCK56-62 (0 to 10 μM final concentration) in the presence of 2 mM GDP and 0.5 nM $[^{35}\text{S}]\text{GTP}\gamma\text{S}$ in 50 mM HEPES buffer containing 5 mM MgCl_2 , 100 mM NaCl, 1 mM EDTA (pH 7.4), and protease inhibitor cocktail. Nonspecific binding was determined in the presence of 10 μM cold $[^{35}\text{S}]\text{GTP}\gamma\text{S}$. Basal values represent values obtained in the presence of GDP and in the absence of ligand. At the end of the incubation period, samples were filtered using a Brandel filtration system and GF/B filters. Filters were washed three times with 3 ml of ice-cold 50 mM Tris-Cl (pH 7.4), and bound radioactivity was measured using a scintillation counter. In a separate set of experiments, membranes (20 μg) from CHO, CHO-GPR83 cells, WT, or GPR83 KO striatum were incubated in the absence or presence of 10 μM (final

concentration) of either PEN18, PEN19, PEN20, PEN22, PEN11-22, PEN11-20, CCK56-63, or CCK56-62.

Adenylate Cyclase Activity Assay. Membranes (2 μg per well) from CHO-GPR83 cells or WT striatum were incubated for 30 minutes at 37°C with either full-length mPEN (PEN22), PEN18, PEN19, PEN20, PEN11-22, PEN11-20, CCK56-63, or CCK56-62 (0 to 10 μM final concentration) in assay buffer (50 mM HEPES, 10 mM MgCl_2 , 100 mM NaCl, 200 μM ATP, 10 μM GTP, pH 7.4) containing 40 μM forskolin, 1X protease inhibitor cocktail, and 100 μM 3-isobutyl-1-methylxanthine, and cAMP levels were measured using the HitHunter cAMP detection kit for membranes from DiscoverRx as described in the manufacturer's protocol. In a separate set of experiments, membranes (2 μg per well) from CHO, CHO-GPR83 cells, and WT or GPR83 KO striatum were incubated in the absence or presence of 10 μM (final concentration) of either PEN18, PEN19, PEN20, PEN22, PEN11-22, PEN11-20, CCK56-63, or CCK56-62. For experiments involving toxins, membranes were preincubated with either pertussis toxin (100 ng/ml) or cholera toxin (100 $\mu\text{g/ml}$) for 15 minutes at room temperature prior to carrying out the assay.

Phospholipase C Assay

Phospholipase C (PLC) activity was measured by incubating membranes from CHO-GPR83 cells or striatum from wild-type mice (10 μg) with either full-length mPEN (PEN22), PEN18, PEN19, or PEN20 (0 to 10 μM final concentration) for 1 hour at 37°C in 0.1 M Tris-Cl buffer (pH 7.4) containing 10 mM CaCl_2 , 80 mM p-nitrophenylphosphorylcholine, and protease inhibitor cocktail (De Silva and Quinn, 1987). The amount of p-nitrophenol released was measured at 410 nm. In a separate set of experiments, membranes (10 μg) from CHO, CHO-GPR83 cells, and WT or GPR83 KO striatum were incubated in the absence or presence of 10 μM (final concentration) of either PEN18, PEN19, PEN20, or PEN22.

Intracellular Ca^{2+} Release Assay

These assays were carried out essentially as described previously (Gomes et al., 2013; Gomes et al., 2016), except that Calcium 6 dye was used instead of Fluo-4 NW. Briefly, CHO-GPR83 cells expressing a chimeric $\text{hG}_{\alpha 15/13}$ protein were plated into black poly-l-lysine-coated 384-well clear-bottom plates (40,000 cells per 25 μl growth media/well). On the next day, cells were incubated with 25 μl Calcium 6 dye in Hanks' balanced salt solution buffer containing protease inhibitor cocktail for 1 hour at 37°C . Cells were then treated with buffer or either full-length mPEN (PEN22), PEN18, PEN19, PEN20 (0 to 10 μM final concentration). Increases in intracellular Ca^{2+} levels were measured for ~ 210 second at excitation 485 nm and emission 525 nm using the FLIPR system. In a separate set of experiments, CHO or CHO-GPR83 cells were incubated in the absence or presence of 10 μM (final concentration) of either PEN18, PEN19, PEN20, or PEN22.

Endocytosis Assay

Receptor endocytosis assays were carried out using previously described protocols (Gupta et al., 2014; Gupta et al., 2015). Briefly, CHO-GPR83 cells were seeded into 24-well plates (2×10^5 cells per well). Cells were labeled with anti-

DYKK monoclonal antibodies (1:1000 in PBS containing 1% FBS) for 1 hour at 4°C and washed three times with growth media, followed by treatment with either full-length mPEN (PEN22), PEN18, PEN19, or PEN20 (0 to 10 μ M final concentration) in media containing protease inhibitor cocktail at 37°C for 1 hour. Cells were briefly fixed (3 minutes) with 4% paraformaldehyde, followed by three washes (5 minutes each) with PBS, followed by incubation with anti-mouse antibody coupled to horseradish peroxidase (1:2000 in PBS containing 1% FBS) for 1 hour at 37°C. Cells were washed three times with 1% FBS in PBS (5 minutes each wash), and color was developed by the addition of the substrate *o*-phenylenediamine [5 mg/10 ml in 0.15-m citrate buffer (pH 5) containing 15 μ l H₂O₂]. Absorbance at 490 nm was measured with a Bio-Rad ELISA reader. For time course experiments, cells were treated with 100 nM of different peptides for different time periods (0-120 minutes).

Data Analysis and Statistics

Data were analyzed using Prism 9.0 software. Data throughout the manuscript is presented as mean plus or minus S.D. Displacement binding assay data (Fig. 2B; Fig. 3A; Fig. 4, B and C; Supplemental Fig. 1, A and I; Supplemental Tables 1 and 3) was analyzed by comparing both one-site-fit logIC₅₀ and two-sites-fit logIC₅₀ curves to determine for each data set which of the two equations fits best. In Fig. 2B, assays with PEN18, PEN19, and PEN20 were carried out three independent times, and with PEN22, six independent times each with triplicate determinations. In Fig. 2C, assays were carried out six independent times each with triplicate determinations. In Fig. 2D, assays were carried out three independent times each with quadruplicate determinations. In Fig. 2E, assays were carried out three independent times each with quadruplicate determinations; data were analyzed using one-way ANOVA with Tukey's multiple comparison. In Fig. 2F, assays were carried out six independent times each with triplicate determinations. In Fig. 2, G–I and Fig. 3, A and B, assays were carried out three independent times each with triplicate determinations. In Fig. 3C, assays were carried out three independent times each with triplicate determinations, and data were analyzed using unpaired *t* test with Welch's correction. In Fig. 3D, assays were carried out three independent times each with quadruplicate determinations. In Fig. 3E, assays were carried out three independent times each with quadruplicate determinations, and data were analyzed using unpaired *t* test with Welch's correction. In Fig. 3F, assays were carried out three independent times each triplicate determinations. In Fig. 4, B–D, assays were carried out six independent times each triplicate determinations. In Fig. 4E, assays were carried out five independent times each triplicate determinations for PEN11-20 and PEN11-22 and three independent times each triplicate determinations for PEN22; data were analyzed using one-way ANOVA with Tukey's multiple comparison. In Fig. 4F, assays were carried out six independent times each triplicate determinations. In Fig. 4G, assays were carried out six independent times each with quadruplicate determinations. In Fig. 4, H and I, assays were carried out four independent times each with quadruplicate determinations. In Supplemental Fig. 1A, assays were carried out six independent times each triplicate determinations. In Supplemental Fig. 1, B and C, assays were carried out six independent times each triplicate determinations; data

were analyzed using two-way ANOVA with Tukey's multiple comparison. In Supplemental Fig. 1, D–F, assays were carried out three independent times each with quadruplicate determinations. In Supplemental Fig. 1G, assays were carried out six independent times each with triplicate determinations; data were analyzed using two-way ANOVA with Tukey's multiple comparison. In Supplemental Fig. 1H, assays were carried out three independent times each with triplicate determinations; data were analyzed using two-way ANOVA with Tukey's multiple comparison. In Supplemental Fig. 1I, assays were carried out three independent times, each with triplicate determinations. In Supplemental Fig. 1J, assays were carried out three independent times each with triplicate determinations; data were analyzed using unpaired *t* test with Welch's correction. In Supplemental Fig. 2A, assays were carried out six independent times each with triplicate determinations; data were analyzed using unpaired *t* test with Welch's correction. In Supplemental Fig. 2B, assays were carried out five independent times each with quadruplicate determinations; data were analyzed using two-way ANOVA with Tukey's multiple comparison. In Supplemental Fig. 2, C and D, assays were carried out five independent times each with quadruplicate determinations. In Supplemental Fig. 2, B–I, assays were carried out four independent times each with quadruplicate determinations.

Results

Binding of C-Terminally Truncated PEN Peptides to Heterologously Expressed GPR83 and Characterization of the Signaling Pathways. We first investigated whether the C-terminally truncated PEN peptides, PEN18, PEN19, and PEN20, (Fig. 2A) can displace [¹²⁵I]Tyr-rPEN binding to membranes from CHO cells stably expressing GPR83 (CHO-GPR83). [¹²⁵I]Tyr-rPEN exhibits robust binding to CHO-GPR83 membranes and not to CHO membranes alone (Supplemental Fig. 1A). Full-length PEN (referred to as "PEN22") as well as PEN18, PEN19, and PEN20 exhibit biphasic displacement binding curves with high affinity in the sub-nM range and low affinity in the high nM - μ M range in CHO-GPR83 membranes (Fig. 2B; Supplemental Fig. 1A; Supplemental Table 1). Moreover, although PEN22 (10 μ M) completely displaces [¹²⁵I]Tyr-PEN binding to CHO-GPR83, this is not the case with PEN18, PEN19, and PEN20, which show only partial displacement (Fig. 2B; Supplemental Table 1).

The pharmacological properties of the C-terminally truncated PEN peptides were characterized using signaling assays previously used to characterize PEN22-GPR83 signaling (Gomes et al., 2016). C-terminally truncated PEN peptides activate G proteins, as measured using the [³⁵S]GTP γ S binding assay, in CHO-GPR83 but not CHO membranes (Supplemental Fig. 1B; Fig. 2C). PEN22 and PEN20 exhibit similar potencies, although PEN20 exhibits a lower but not statistically significant difference in efficacy ($118 \pm 3\%$) compared with PEN22 ($126 \pm 3\%$) (Fig. 2C; Supplemental Table 2). PEN19 was less potent (777 ± 2 nM) and less efficacious ($111 \pm 4\%$) than PEN22, and PEN18 could not induce increases in [³⁵S]GTP γ S binding (Fig. 2C; Supplemental Table 2). Since the GTP γ S binding assay primarily detects G α i proteins (Harrison and Traynor, 2003), these results do not rule out the possibility that PEN18 and PEN19 could signal via other G α proteins. To investigate whether C-terminally truncated PEN peptides signal through G α s or G α i, we used the

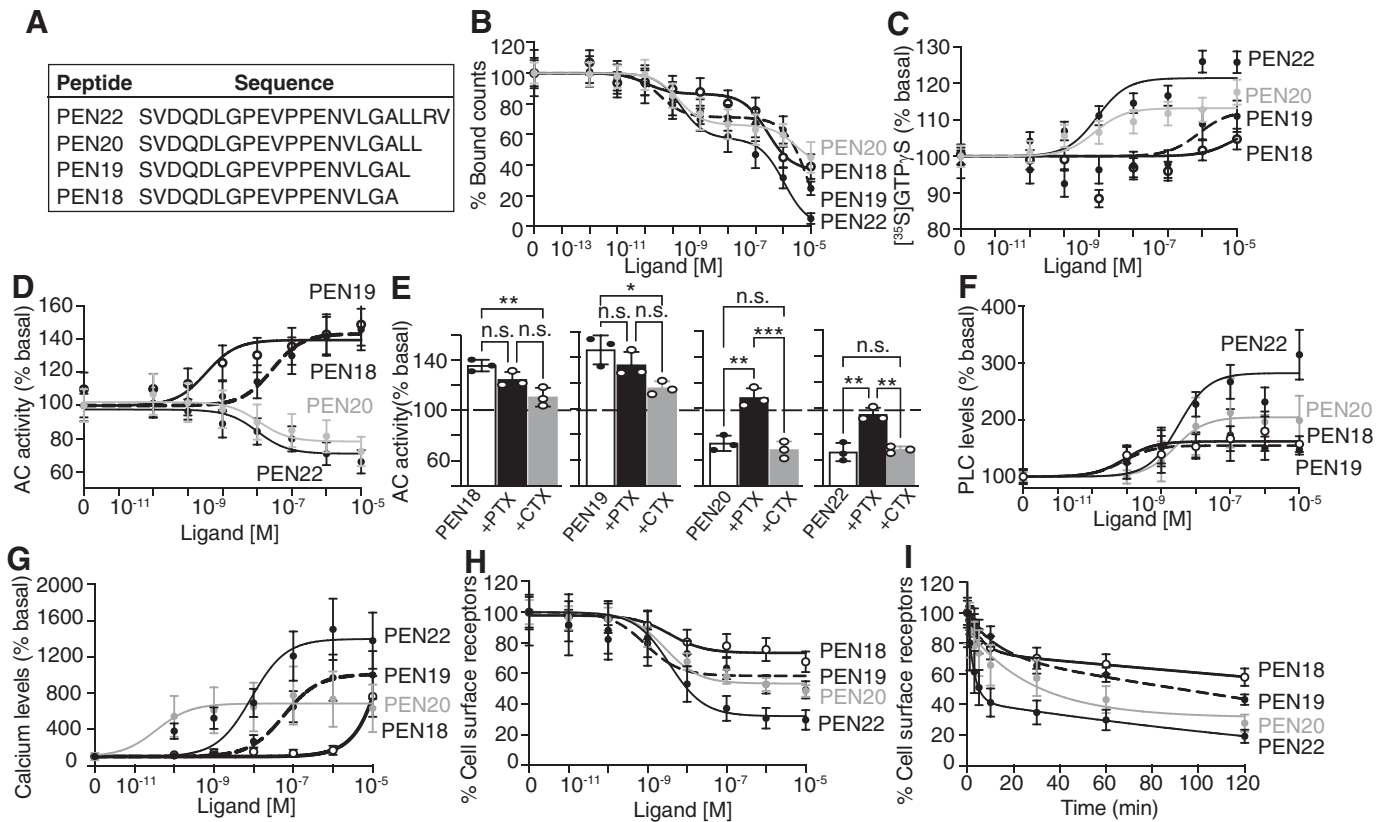


Fig. 2. Binding and signaling by C-terminally truncated PEN peptides at CHO-GPR83. (A) Sequence of full-length PEN (PEN22) and of the C-terminally truncated peptides, PEN18, PEN19, and PEN20. (B) C-terminally truncated PEN peptides displace [¹²⁵I]-Tyr-rPEN binding (3 nM) to membranes (20 μg) from CHO cells expressing GPR83 (CHO-GPR83). Data represent mean plus or minus S.D. (n = 3 for PEN18, PEN19, and PEN20 and n = 6 for PEN22). (C) C-terminally truncated PEN peptide-mediated increases in [³⁵S]GTPγS binding to CHO-GPR83 membranes (20 μg). Data represent mean plus or minus S.D. (n = 6). (D) Modulation of adenylyl cyclase activity by C-terminally truncated PEN peptides in CHO-GPR83 membranes (2 μg). Data represent mean plus or minus S.D. (n = 3). (E) Effect of pertussis toxin (PTX) and cholera toxin (CTX) treatment on PEN18-, PEN19-, PEN20-, and PEN22-mediated inhibition of adenylyl cyclase activity. Data represent mean plus or minus S.D. (n = 3). **P* < 0.05; ***P* < 0.01; ****P* < 0.001 (one-way ANOVA with Tukey's multiple comparison). (F) C-terminally truncated PEN peptide-mediated changes in phospholipase C activity in CHO-GPR83 cell membranes. Data represent mean plus or minus S.D. (n = 6). (G) C-terminally truncated PEN peptide-mediated increases in intracellular Ca²⁺ levels in CHO-GPR83 cells. Data represent mean plus or minus S.D. (n = 3). (H) Dose-dependent modulation of GPR83 endocytosis by C-terminally truncated PEN peptides. (I) Time course of GPR83 internalization by C-terminally truncated PEN peptides. Data (H-I) represent mean plus or minus S.D. (n = 3). n.s., not significant.

adenylyl cyclase activity assay. C-terminally truncated PEN peptides modulated adenylyl cyclase activity in CHO-GPR83 but not CHO membranes (Supplemental Fig. 1C). Treatment of CHO-GPR83 cell membranes with PEN22 or PEN20 led to a dose-dependent decrease in adenylyl cyclase activity, and this could be blocked by pertussis toxin (Fig. 2, D and E; Supplemental Fig. 1; Supplemental Table 2). Interestingly, PEN18 or PEN19 treatment led to a dose-dependent increase in adenylyl cyclase activity that could be substantially attenuated by cholera toxin treatment (Fig. 2, D and E; Supplemental Fig. 1; Supplemental Table 2). Taken together, these results are consistent with the notion that PEN22 and PEN20 facilitate Gα_i-mediated signaling while PEN18 and PEN19 facilitate Gα_s-mediated signaling by engaging GPR83, suggesting biased signaling by endogenous C-terminally truncated PEN peptides.

PEN22 was previously shown to exhibit both Gα_q- and Gα_i-mediated signaling at GPR83 (Gomes et al., 2016). We therefore examined the ability of C-terminally truncated PEN peptides to signal via Gα_q proteins using the PLC assay and also by measuring their ability to increase intracellular Ca²⁺ levels. C-terminally truncated PEN peptides increase

PLC activity in CHO-GPR83 but not CHO membranes (Supplemental Fig. 1G) with sub-nM to nM potency (Fig. 2F; Supplemental Table 2). However, they differ in their efficacy in CHO-GPR83 membranes, with PEN22 being the most efficacious and PEN18 and PEN19 the least efficacious (Fig. 2F; Supplemental Table 2). C-terminally truncated PEN peptides increase intracellular Ca²⁺ levels in CHO-GPR83 but not CHO cells (Supplemental Fig. 1H). In CHO-GPR83 cells, treatment with PEN19 or PEN20 increased intracellular Ca²⁺ levels, although with much lesser efficacy than PEN22, whereas PEN18 treatment caused an increase only at the highest concentration tested (10 μM) (Fig. 2G; Supplemental Table 2). These results are consistent with the notion that C-terminally truncated PEN peptides can also signal via Gα_q proteins, thereby suggesting the promiscuity of Gα protein subtype coupling by GPR83.

Exposure to agonists often leads to endocytosis of G protein-coupled receptors (GPCRs), which can modulate cellular responses (Lobingier and von Zastrow, 2019). Therefore, we looked at the ability of C-terminal-truncated PEN peptides to induce GPR83 endocytosis. These peptides cause a dose- and time-dependent endocytosis of GPR83, although there are

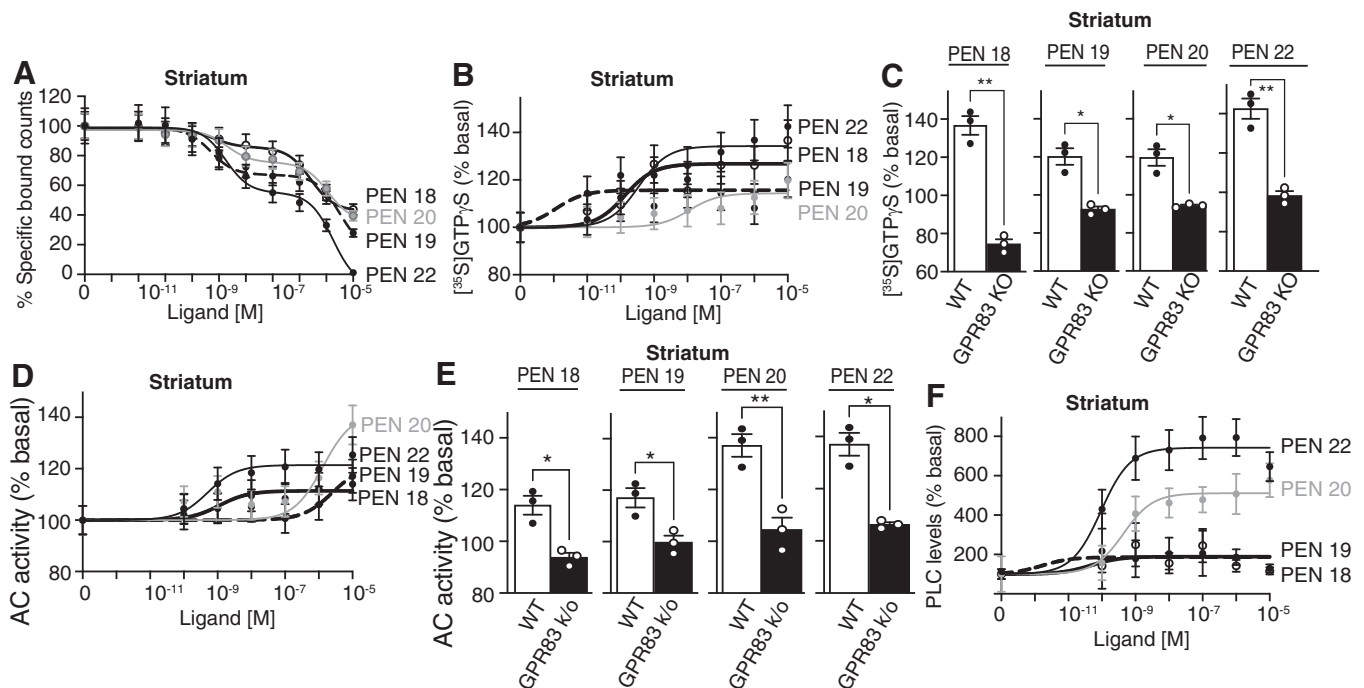


Fig. 3. Binding and signaling by C-terminally truncated PEN peptides at striatal membranes. (A) C-terminally truncated PEN peptides displace $[^{125}\text{I}]\text{-Tyr-PEN}$ binding (3 nM) to striatal membranes (20 μg). Data represent mean plus or minus S.D. ($n = 3$). (B and C) C-terminally truncated PEN peptide-mediated increases in $[^{35}\text{S}]\text{GTP}\gamma\text{S}$ binding to striatal membranes (20 μg) from wild-type (B and C) and GPR83 knockout (C) mice. Data represent mean plus or minus S.D. ($n = 3$). In (C), $*P < 0.05$; $**P < 0.01$; WT versus GPR83 KO; unpaired t test with Welch's correction. (D and E) Modulation of adenylyl cyclase activity by C-terminally truncated PEN peptides in striatal membranes (2 μg) from WT (D and E) and GPR83 KO (E) mice. Data represent mean plus or minus S.D. ($n = 3$). In (E), $*P < 0.05$; $**P < 0.01$; WT versus GPR83 KO; unpaired t test with Welch's correction. (F) C-terminally truncated PEN peptide-mediated changes in phospholipase C activity in striatal membranes (10 μg). Data represent mean plus or minus S.D. ($n = 3$).

differences in the extent of receptor endocytosis as compared with PEN22 (Fig. 2, H and I; Supplemental Table 2). At a highest concentration (10 μM), PEN18 induces $\sim 32\%$, PEN19 and PEN20 $\sim 51\%$, and PEN22 $\sim 70\%$ receptor endocytosis (Fig. 2H; Supplemental Table 2). Even after prolonged exposure to these peptides (2 hours), we find that PEN18 is the least effective at inducing GPR83 endocytosis (Fig. 2I; Supplemental Table 2). Taken together, these results show that C-terminally truncated PEN peptides exhibit differential signaling and endocytosis of GPR83.

Binding of C-Terminally Truncated PEN Peptides to Striatal GPR83 and Characterization of the Signaling Pathways. First, we examined $[^{125}\text{I}]\text{Tyr-rPEN}$ binding to WT and GPR83 KO striatal membranes and found robust binding with WT but not GPR83 KO membranes (Supplemental Fig. 1I). Next, we examined if C-terminally truncated PEN peptides could bind to and signal through native GPR83 in the striatum. As found with the cell line studies described above, all of the PEN peptides exhibit biphasic displacement binding curves with high-affinity binding in the sub-nM range and low-affinity binding in the high nM- μM range (Fig. 3A; Supplemental Table 1). C-terminally truncated PEN peptides in striatal membranes induce dose-dependent increases in $[^{35}\text{S}]\text{GTP}\gamma\text{S}$ binding (Fig. 3B; Supplemental Table 2). Like PEN22, the peptides exhibit nM potencies but differ in their efficacies, with PEN19 and PEN20 being least efficacious (Fig. 3B; Supplemental Table 2). This signaling appears to be mediated through GPR83 based on the finding that peptide-mediated increases in $[^{35}\text{S}]\text{GTP}\gamma\text{S}$ binding are not seen in GPR83 KO striatal membranes (Fig. 3C). In the

adenylyl cyclase activity assays, PEN18 and PEN19 cause modest increases in activity, whereas treatment with PEN20 and PEN22 cause robust increases (Fig. 3D; Supplemental Table 2). These increases in activity were abrogated in GPR83 KO striatal membranes (Fig. 3E). In the phospholipase C activity assay, the peptides cause dose-dependent increases in activity (Fig. 3F; Supplemental Table 2), with more robust effects being observed with PEN20 and PEN22 compared with PEN18 and PEN19 (Fig. 3F; Supplemental Table 2); these increases in activity were not seen in GPR83 KO striatal membranes (Supplemental Fig. 1J). Together, these results show that C-terminal-truncated PEN peptides can bind to and signal through GPR83 in the striatum. Moreover, the peptides can elicit $\text{G}\alpha_i$, $\text{G}\alpha_s$, and $\text{G}\alpha_q$ -mediated signaling in this brain region.

Binding of Procholecystokinin-Derived Peptides to GPR83 and Characterization of the Signaling Pathways. Based on the finding that PEN20 and other related peptides bound to and signaled through GPR83, it was of interest to test the proCCK peptide that shares the C-terminal sequence with PEN20 (i.e., CCK56-62) (Fig. 1). In addition, another frequently detected peptide that contains one additional C-terminal residue was also examined (i.e., CCK56-63) (Fig. 1). Synthetic peptides representing the C-terminal region of two PEN peptides (i.e., PEN11-20 and PEN11-22) were included in the analysis for comparison (Fig. 4A). Both of the proCCK peptides as well as the shorter PEN peptides displaced $[^{125}\text{I}]\text{Tyr-PEN}$ binding to CHO-GPR83 cell membranes (Fig. 4B; Supplemental Table 3) and striatal membranes (Fig. 4C; Supplemental Table 3), showing biphasic

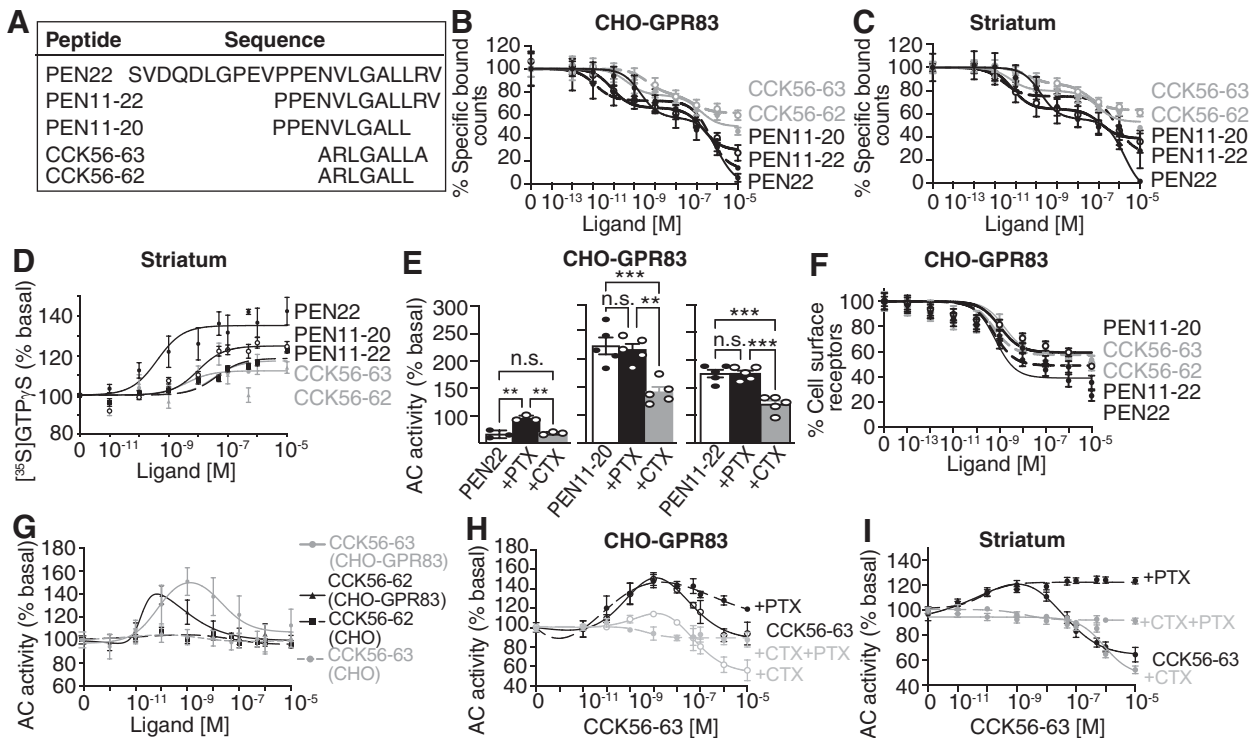


Fig. 4. Binding and signaling by proCCK-derived peptides at CHO-GPR83. (A) Sequence of proCCK-derived peptides that exhibit similarity to peptides derived from PEN 22 (PEN11-20 and PEN11-22). (B and C) ProCCK-derived peptides and related PEN peptides displace [125 I]-Tyr-PEN binding (3 nM) to membranes (20 μ g) from CHO-GPR83 (B) and WT striatum (C). Data represent mean plus or minus S.D. (n = 6). (D) ProCCK-derived peptide- and related PEN peptide-mediated increases in [35 S]GTP γ S binding to striatal membranes (20 μ g). Data represent mean plus or minus S.D. (n = 6). (E) PEN11-20 and PEN11-22-mediated increase in adenylyl cyclase activity in CHO-GPR83 cell membranes is blocked by CTX but not by PTX. Data represent mean plus or minus S.D. (n = 5 for PEN11-20 and PEN11-22 and n = 3 for PEN22). ** P < 0.01; *** P < 0.001 (one-way ANOVA with Tukey's multiple comparison test). (F) GPR83 endocytosis by proCCK-derived peptides and related PEN peptides in CHO-GPR83 cells. Data represent mean plus or minus S.D. (n = 6). (G) Modulation of adenylyl cyclase activity by proCCK-derived peptides in CHO and in CHO-GPR83 membranes (2 μ g). Data represent mean plus or minus S.D. (n = 6). (H and I) A combination of CTX and PTX is needed to block CCK56-63-mediated changes in adenylyl cyclase activity in CHO-GPR83 (H) and striatal (I) membranes. Data represent mean plus or minus S.D. (n = 4).

displacement profiles with high-affinity binding in the sub-nM range and low-affinity binding in the high nM range. All of these peptides also induce robust increases in [35 S]GTP γ S binding in WT striatal membranes, although they are less potent and less efficacious than PEN22 (Fig. 4D; Supplemental Table 4). The increases in [35 S]GTP γ S binding caused by treatment with CCK56-62 and CCK56-63 are substantially reduced in GPR83 KO striatal membranes (Supplemental Fig. 2A). Together, these results support the idea that the "LGALL" motif common to all of the peptides is responsible for binding to GPR83.

Next, we examined if PEN11-20, PEN11-22, CCK56-62, and CCK56-63 exhibit differences in downstream signaling. In the adenylyl cyclase activity assay, PEN11-20 and PEN11-22 exhibit increases in activity in CHO-GPR83 but not CHO membranes (Supplemental Fig. 2, B–D; Supplemental Table 4); these increases are blocked by pretreatment with cholera toxin but not pertussis toxin (Fig. 4E; Supplemental Fig. 2, C and D), indicating that these peptides activate G α s-mediated signaling. In contrast, CCK56-62 and CCK56-63 exhibit a bell-shaped profile of adenylyl cyclase activity with a peak in the sub-nM to nM range (Fig. 4G; Supplemental Fig. 2; Supplemental Table 4); the peptides have no effects on adenylyl cyclase activity in CHO cell membranes (Fig. 4G). Pretreatment with cholera toxin attenuates CCK56-62- or CCK56-63-mediated adenylyl cyclase activity seen at low doses (0.1 to 10 nM), whereas pertussis toxin treatment

attenuates the activity seen at higher doses of the peptides, and a combination of both toxins completely abrogates signaling by both peptides (Fig. 4, H and I; Supplemental Fig. 2). Moreover, PEN11-20, PEN11-22, CCK56-62, and CCK56-63 induce GPR83 endocytosis with a potency in the nM range (Fig. 4F; Supplemental Table 4). These results indicate that the proCCK peptides that share sequence identity with PEN can bind to and differentially signal at GPR83 in a dose-dependent manner. Taken together our results show that PEN binding and signaling through GPR83 is largely mediated by the C-terminal portion of the peptide, that GPR83 is activated by peptides from proCCK (in addition to proSAAS), and this leads to differential signaling, allowing for fine tuning of GPR83 signaling.

Discussion

Our findings expand the repertoire of endogenous GPR83 ligands and highlight the complexities of this neuropeptide-receptor signaling system. One major finding is that C-terminal-truncated PEN-derived peptides can bind and signal through GPR83. These truncated peptides appear to be major forms of PEN in brain and other tissues (Mzhavia et al., 2001; Mzhavia et al., 2002; Fricker, 2010). Rather than representing inactive degradation fragments, we find that the truncated peptides exhibit differences in their abilities to activate downstream signaling pathways, a phenomenon commonly referred to as

“biased agonism.” There are several other examples of biased GPCR signaling arising from small differences in a peptide’s length. For example, binding of angiotensin II to angiotensin receptors triggers G protein-mediated signaling while the binding of a peptide that is one amino acid shorter (Ang₁₋₇) leads to β -arrestin-mediated signaling (Teixeira et al., 2017). Other examples of this phenomenon are found with opioid peptides, where pentapeptide enkephalins and C-terminally extended enkephalins show differences in G protein versus β -arrestin signaling at μ , δ , and κ opioid receptors (Gomes et al., 2020). The present findings that various PEN peptides show biased signaling through GPR83 extends this phenomenon and implies that the peptidases that convert PEN22 into shorter peptides produce a subtle change in the signaling profiles.

Another major finding of the present study is that proCCK-derived peptides bind and signal via GPR83, although this does not rule out that the peptides could also signal via an as yet unidentified receptor since residual signaling is detected in GPR83 KO striatal membranes (Supplemental Fig. 2A). At GPR83, these peptides activate G α s-mediated signaling at low concentrations (≤ 1 nM) and G α i-mediated signaling at higher concentrations. This supports our observations that GPR83 can signal via G α s, G α i and G α q proteins (Gomes et al., 2016), and extends the dynamics of signaling by endogenous peptides. It has been reported that neuropeptide Y and other agonists of the type-2 neuropeptide Y receptor bind to GPR83 (Sah et al., 2007). However, another study found that high concentrations of neuropeptide Y caused only a small displacement in [¹²⁵I]Tyr-PEN binding to human GPR83, suggesting that the binding site for the two peptides may be distinct (Gomes et al., 2016). A recent study reported that FAM237A and, to a lesser extent, FAM237B peptides induce β -arrestin recruitment and inositol phosphate recruitment via GPR83, although the authors were not able to detect consistent changes in cAMP levels (Sallee et al., 2020). Finally, the basal activity of GPR83 has been reported to be modulated by the N-terminal domain of the receptor and by Zn²⁺ (Muller et al., 2013a; Muller et al., 2016). Together, these findings suggest that the activity of GPR83 can be regulated by different modalities. However, only the activation of GPR83 by PEN has been replicated by independent investigators (Foster et al., 2019; Parobchak et al., 2020), which is a criterion for “deorphanizing” a receptor. The other reported ligands (including the proCCK peptides in the present study) await confirmation.

If CCK56-62 and CCK56-63 serve as endogenous GPR83 ligands, these peptides should be secreted in the vicinity of cells expressing GPR83. High levels of proCCK mRNA are expressed in the cortex, hippocampus, thalamus, and several other regions. In contrast, GPR83 mRNA is highly expressed in nucleus accumbens, caudoputamen, and olfactory tubercle as well as specific nuclei in other regions (Fig. 5). Because neuropeptides can be secreted from nerve terminals located far from the cell bodies where their mRNA is expressed, it is important to consider neuronal projections. GPR83 is expressed on interneurons in the striatum that receive direct inputs from various regions where proCCK is expressed (Klug et al., 2018; Fakira et al., 2019; Enterria-Morales et al., 2020). Cortico-striatal projections directly release proCCK peptides into the striatum (Schiffmann and Vanderhaeghen, 1991; Morino et al., 1994; You et al., 1994). ProCCK mRNA is also expressed in thalamostriatal projections (Burgunder and Young, 1988),

providing an additional source of proCCK peptides in the striatum. Neurons in the ventral tegmental area and substantia nigra pars compacta have also been shown to release CCK into the striatum and olfactory tubercle (Hokfelt et al., 1980b; Zaborszky et al., 1985). In addition, it is possible that GPR83 expressed in the cortex is activated by proCCK peptides released from cortical interneurons (Pesini et al., 1998; Brezillon et al., 2001; Wang et al., 2001; Adams et al., 2003; Whissell et al., 2015; Lueptow et al., 2018; Nguyen et al., 2020). Taken together, it is likely that proCCK56-62 and related peptides are secreted in the proximity of GPR83.

The brain regions expressing high levels of proCCK mRNA are distinct from those expressing high levels of proSAAS (Fig. 5). Little is known regarding projections of proSAAS-expressing neurons, but due to the broad expression of low levels of proSAAS throughout the brain, it is likely that GPR83 is exposed to secreted PEN and related peptides. In the brain, GPR83 is likely to integrate signals from a broad range of brain areas, with cortical-striatal projections releasing proCCK peptides and projections from other regions releasing PEN. Recently, GPR83 was reported to be expressed on neurons that project from the spinal cord to the lateral parabrachial nucleus of the pons, a region that represents a major ascending spinal pathway for processing of tactile and noxious stimuli (Choi et al., 2020). Both proSAAS and proCCK are abundantly expressed in the spinal cord, and thus, both PEN and proCCK peptides are potential ligands for GPR83 in this tissue (Larsson and Rehfeld, 1979; Feng et al., 2001; Chakraborty et al., 2006; Royds et al., 2020).

The vast majority of previous reports on proCCK-derived peptides have focused on CCK-containing peptides, which includes a number of N-terminally extended peptides (Fig. 1). The peptide CCK56-63 is cleaved from proCCK at single basic cleavage sites Arg55 and Arg64. Cleavage of proCCK at Arg 64 generates a long form of CCK designated CCK39 (Rehfeld et al., 2007). Although the Arg55 cleavage site on the N-terminus of CCK56-63 does not appear to have been previously reported in the CCK field, another site further upstream (Arg45) produces the long CCK form named CCK58 (Rehfeld et al., 2007). Interestingly, intraperitoneal injections of synthetic CCK58 or CCK8 produced comparable reductions of meal size, but CCK58 increased the satiety ratio, and this effect was not seen with CCK8 (Overduin et al., 2014; Sayegh et al., 2014). If CCK58 activates GPR83, this could potentially account for the additional effects seen with the longer peptide. Although this was not directly tested in the present study, our finding that CCK56-62 and CCK56-63 produce similar effects indicate that the LGALL motif does not need to be at the extreme C-terminus of the peptide to activate GPR83, raising the possibility that CCK58 also activates this receptor. If this prediction is confirmed, it could potentially explain the different biologic effects of CCK8 and CCK58 observed by Reeve and colleagues (Overduin et al., 2014; Sayegh et al., 2014).

Some of the peptidases that generate the various peptides described in the present study can be predicted based on previous peptidomic studies on mice lacking specific peptide-processing enzymes. Cleavage at Arg45 and Arg64 produces the peptide CCK46-63, which was detected many times in mouse brain peptidomics studies (Fricker, 2010). This peptide and the shorter CCK56-63 used in the present study are

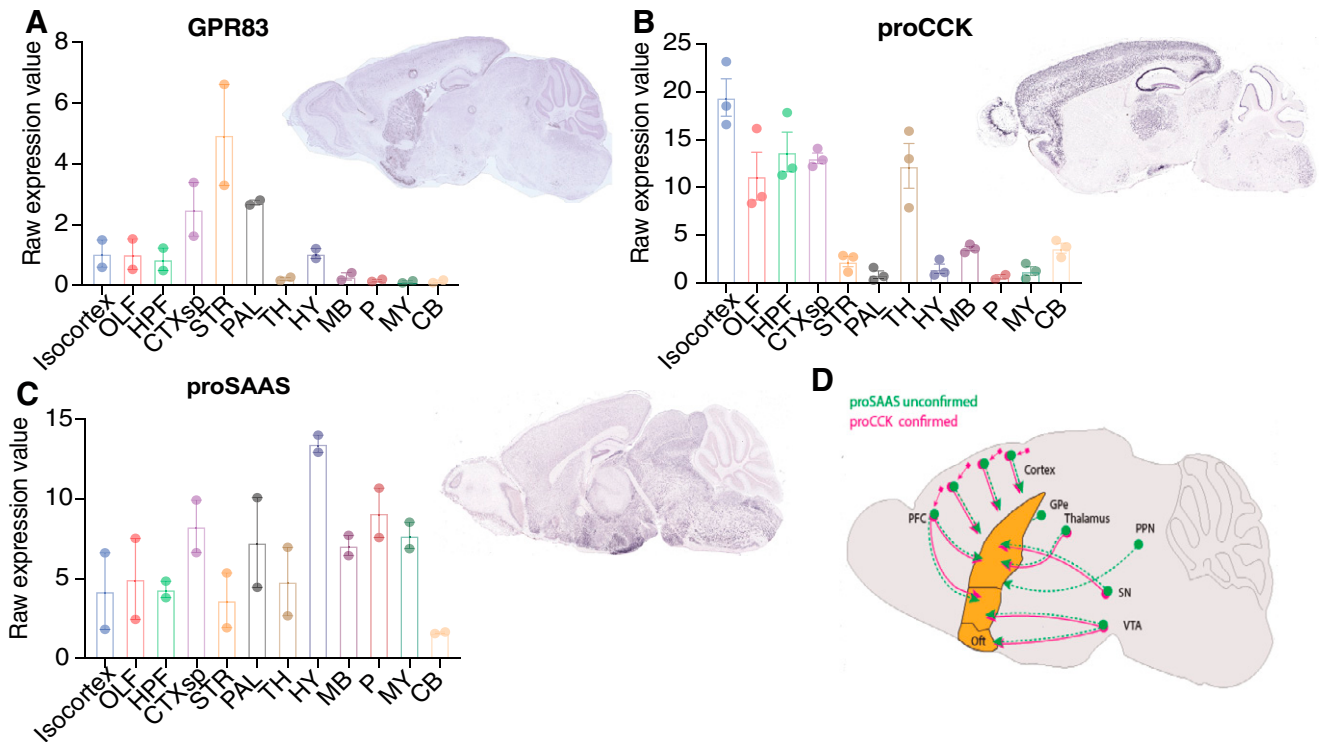


Fig. 5. Characterization of GPR83, proSAAS, and proCCK brain distribution in mice. The data for the mRNA expression was obtained from Allen Brain Mouse Atlas (<https://mouse.brain-map.org/experiment>), which shows in situ hybridization of sagittal mouse brain sections probed with GPR83 (A), proCCK (B), and proSAAS (gene name *Pcsk1n*) (C). Bar graphs represent the average raw expression value for different brain regions; each dot represents a biologic replicate. D. Diagram showing potential projections of proCCK- and proSAAS-derived neuropeptide release into brain regions with high levels of GPR83 expression. Projections of proCCK neurons and the expression of proSAAS-derived peptides were obtained from previous studies (Burgunder and Young, 1988; Schiffmann and Vanderhaeghen, 1991; Morino et al., 1994; You et al., 1994; Pesini et al., 1998; Brezillon et al., 2001; Wang et al., 2001; Adams et al., 2003; Whissell et al., 2015; Lueptow et al., 2018; Nguyen et al., 2020). Solid pink arrows represent the proCCK neuronal projections to striatum and olfactory tubercle (orange), both of which express GPR83 mRNA. Dashed green lines represent projections to the striatum and olfactory tubercle that express proSAAS mRNA, and these are potential sources of PEN in the GPR83-rich brain regions. CB, cerebellum; CTXsp, cortical subplate; HPF, hippocampal formation; HY, hypothalamus; MB, midbrain; MY, medulla; OLF, olfactory area; P, pons; PAL, pallidum; STR, striatum; TH, thalamus.

both produced in the late secretory pathway by CPE, based on peptidomics analyses of *Cpe*-null mice (Lim et al., 2006; Zhang et al., 2008). CCK56-63 is produced from CCK46-63 by prohormone convertase 2, based on the changes observed in *Pcsk2*-null mice (Pan et al., 2006; Zhang et al., 2010). C-terminally truncated forms were detected many times in mouse brain, including CCK46-62 (ending with LGALL), as well as shorter C-terminally truncated forms that were not tested in the present study. Similarly, PEN22 and shorter forms have been frequently detected in mouse brain and in proSAAS-expressing cell lines (Mzhavia et al., 2001; Mzhavia et al., 2002; Fricker, 2010). PEN22 is produced from proSAAS mainly via furin acting at the consensus sites RxRR on either side of PEN22, followed by removal of the C-terminal R residues by carboxypeptidase D. In contrast, PEN20 is produced later in the secretory pathway and requires CPE for its formation, based on the absence of this peptide in *Cpe*-null mice (Lim et al., 2006; Zhang et al., 2008). It is not clear if the C-terminal trimming of PEN20 and CCK56-63 into shorter peptides occurs within secretory granules or by extracellular enzymes following secretion of the peptides.

Taken together, this study sheds light on the complexity of the GPR83 signaling system and raises the exciting and intriguing possibility of exploiting the potential biased signaling at GPR83 to develop therapeutics targeting this receptor

for the treatment of obesity, addiction, and reward-related disorders.

Authorship Contributions

Participated in Research Design: Mack, Gomes, Fakira, Fricker, Devi.

Conducted Experiments: Mack, Gomes, Fakira, Duarte, Gupta.

Performed data analysis: Mack, Gomes, Fakira.

Wrote or contributed to the writing to the manuscript: Mack, Gomes, Fakira, Fricker, Devi.

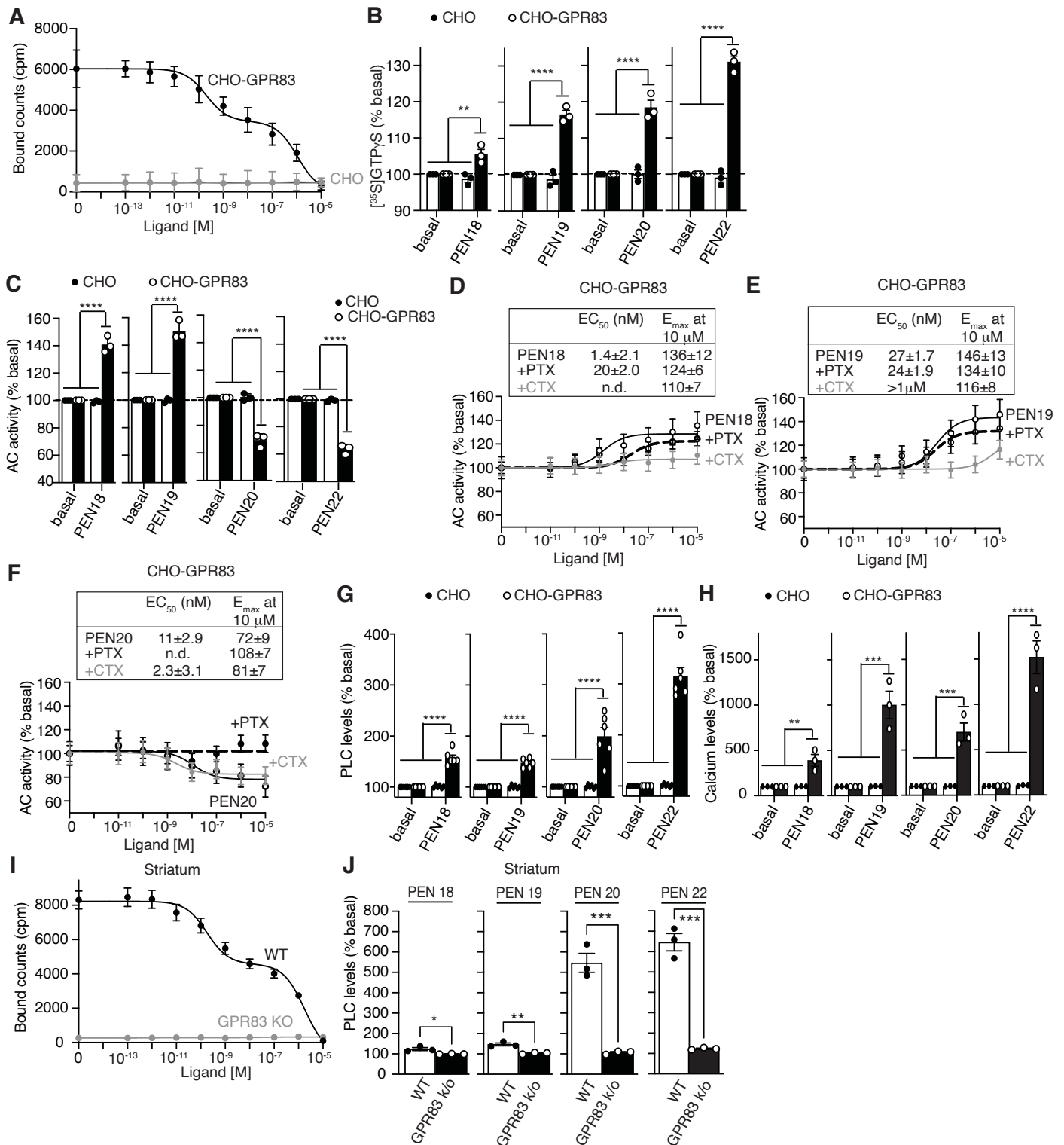
References

- Adams F, Grassie M, Shahid M, Hill DR, and Henry B (2003) Acute oral dexamethasone administration reduces levels of orphan GPCR glucocorticoid-induced receptor (GIR) mRNA in rodent brain: potential role in HPA-axis function. *Brain Res Mol Brain Res* 117:39–46.
- Beinfeld MC (2003) Biosynthesis and processing of pro CCK: recent progress and future challenges. *Life Sci* 72:747–757.
- Brezillon S, Detheux M, Parmentier M, Hökfelt T, and Hurd YL (2001) Distribution of an orphan G-protein coupled receptor (JP05) mRNA in the human brain. *Brain Res* 921:21–30.
- Burgunder JM and Young 3rd WS (1988) The distribution of thalamic projection neurons containing cholecystokinin messenger RNA, using in situ hybridization histochemistry and retrograde labeling. *Brain Res* 464:179–189.
- Chakraborty TR, Tkalych O, Nanno D, Garcia AL, Devi LA, and Salton SR (2006) Quantification of VGF- and pro-SAAS-derived peptides in endocrine tissues and the brain, and their regulation by diet and cold stress. *Brain Res* 1089:21–32.
- Choi S, Hachisuka J, Brett MA, Magee AR, Omori Y, Iqbal NU, Zhang D, DeLisle MM, Wolfson RL, Bai L, et al. (2020) Parallel ascending spinal pathways for affective touch and pain. *Nature* 587:258–263.

- De Silva NS and Quinn PA (1987) Rapid screening assay for phospholipase C activity in mycoplasmas. *J Clin Microbiol* **25**:729–731.
- Enterria-Morales D, Del Rey NL, Blesa J, López-López I, Gallet S, Prévot V, López-Barneo J, and d'Anglemont de Tassigny X (2020) Molecular targets for endogenous glial cell line-derived neurotrophic factor modulation in striatal parvalbumin interneurons. *Brain Commun* **2**:fcaa105.
- Fakira AK, Lueptow LM, Trimbake NA, and Devi LA (2021) PEN receptor GPR83 in anxiety-like behaviors: differential regulation in global vs amygdala knockdown. *Front Neurosci* **15**:675769.
- Fakira AK, Peck EG, Liu Y, Lueptow LM, Trimbake NA, Han MH, Calipari ES, and Devi LA (2019) The role of the neuropeptide PEN receptor, GPR83, in the reward pathway: Relationship to sex-differences. *Neuropharmacology* **157**:107666.
- Feng Y, Reznik SE, and Fricker LD (2001) Distribution of proSAAS-derived peptides in rat neuroendocrine tissues. *Neuroscience* **105**:469–478.
- Foster SR, Hauser AS, Vedel L, Strachan RT, Huang XP, Gavin AC, Shah SD, Nayak AP, Haugard-Kedström LM, Penn RB, et al. (2019) Discovery of human signaling systems: pairing peptides to G protein-coupled receptors. *Cell* **179**:895–908.e21.
- Fricker LD (2010) Analysis of mouse brain peptides using mass spectrometry-based peptidomics: implications for novel functions ranging from non-classical neuropeptides to microproteins. *Mol Biosyst* **6**:1355–1365.
- Fricker LD, Margolis EB, Gomes I, and Devi LA (2020) Five Decades of Research on Opioid Peptides: Current Knowledge and Unanswered Questions. *Mol Pharmacol* **98**:96–108.
- Fricker LD, McKinzie AA, Sun J, Curran E, Qian Y, Yan L, Patterson SD, Courchesne PL, Richards B, Levin N, et al. (2000) Identification and characterization of proSAAS, a granin-like neuroendocrine peptide precursor that inhibits prohormone processing. *J Neurosci* **20**:639–648.
- Goetze JP and Rehfeld JF (2019) Procholecystokinin expression and processing in cardiac myocytes. *Peptides* **111**:71–76.
- Gomes I, Aryal DK, Wardman JH, Gupta A, Gagnidze K, Rodriguez RM, Kumar S, Wetzel WC, Pintar JE, Fricker LD, et al. (2013) GPR171 is a hypothalamic G protein-coupled receptor for BigLEN, a neuropeptide involved in feeding. *Proc Natl Acad Sci USA* **110**:16211–16216.
- Gomes I, Bobeck EN, Margolis EB, Gupta A, Sierra S, Fakira AK, Fujita W, Müller TD, Müller A, Tschöp MH, et al. (2016) Identification of GPR83 as the receptor for the neuroendocrine peptide PEN. *Sci Signal* **9**:ra43.
- Gomes I, Sierra S, Lueptow L, Gupta A, Gouty S, Margolis EB, Cox BM, and Devi LA (2020) Biased signaling by endogenous opioid peptides. *Proc Natl Acad Sci USA* **117**:11820–11828.
- Gupta A, Fujita W, Gomes I, Bobeck E, and Devi LA (2015) Endothelin-converting enzyme 2 differentially regulates opioid receptor activity. *Br J Pharmacol* **172**:704–719.
- Gupta A, Gomes I, Wardman J, and Devi LA (2014) Opioid receptor function is regulated by post-endocytic peptide processing. *J Biol Chem* **289**:19613–19626.
- Harrigan MT, Baughman G, Campbell NF, and Bourgeois S (1989) Isolation and characterization of glucocorticoid- and cyclic AMP-induced genes in T lymphocytes. *Mol Cell Biol* **9**:3438–3446.
- Harrigan MT, Campbell NF, and Bourgeois S (1991) Identification of a gene induced by glucocorticoids in murine T-cells: a potential G protein-coupled receptor. *Mol Endocrinol* **5**:1331–1338.
- Harrison C and Traynor JR (2003) The [35S]GTPgammaS binding assay: approaches and applications in pharmacology. *Life Sci* **74**:489–508.
- Hökfelt T, Skirboll L, Rehfeld JF, Goldstein M, Markey K, and Dann O (1980b) A subpopulation of mesencephalic dopamine neurons projecting to limbic areas contains a cholecystokinin-like peptide: evidence from immunohistochemistry combined with retrograde tracing. *Neuroscience* **5**:2093–2124.
- Klug JR, Engelhardt MD, Cadman CN, Li H, Smith JB, Ayala S, Williams EW, Hoffman H, and Jin X (2018) Differential inputs to striatal cholinergic and parvalbumin interneurons imply functional distinctions. *eLife* **7**:e35657.
- Larsson LI and Rehfeld JF (1979) Localization and molecular heterogeneity of cholecystokinin in the central and peripheral nervous system. *Brain Res* **165**:201–218.
- Lim J, Berezniuk I, Che FY, Parikh R, Biswas R, Pan H, and Fricker LD (2006) Altered neuropeptide processing in prefrontal cortex of Cpe (fat/fat) mice: implications for neuropeptide discovery. *J Neurochem* **96**:1169–1181.
- Lobingier BT and von Zastrow M (2019) When trafficking and signaling mix: How subcellular location shapes G protein-coupled receptor activation of heterotrimeric G proteins. *Traffic* **20**:130–136.
- Lueptow LM, Devi LA, and Fakira AK (2018) Targeting the Recently Deorphanized Receptor GPR83 for the Treatment of Immunological, Neuroendocrine and Neuropsychiatric Disorders. *Prog Mol Biol Transl Sci* **159**:1–25.
- Mack SM, Gomes I, and Devi LA (2019) Neuropeptide PEN and Its Receptor GPR83: Distribution, Signaling, and Regulation. *ACS Chem Neurosci* **10**:1884–1891.
- Morino P, Herrera-Marschitz M, Castel MN, Ungerstedt U, Varro A, Dockray G, and Hökfelt T (1994) Cholecystokinin in cortico-striatal neurons in the rat: immunohistochemical studies at the light and electron microscopic level. *Eur J Neurosci* **6**:681–692.
- Müller A, Berkmann JC, Scheerer P, Biebermann H, and Kleinau G (2016) Insights into Basal Signaling Regulation, Oligomerization, and Structural Organization of the Human G-Protein Coupled Receptor 83. *PLoS One* **11**:e0168260.
- Müller A, Kleinau G, Piechowski CL, Müller TD, Finan B, Pratzka J, Grütters A, Krude H, Tschöp M, and Biebermann H (2013a) G-protein coupled receptor 83 (GPR83) signaling determined by constitutive and zinc(II)-induced activity. *PLoS One* **8**:e53347.
- Müller TD, Müller A, Yi CX, Habegger KM, Meyer CW, Gaylinn BD, Finan B, Heppner K, Trivedi C, Bielohuby M, et al. (2013b) The orphan receptor Gpr83 regulates systemic energy metabolism via ghrelin-dependent and ghrelin-independent mechanisms. *Nat Commun* **4**:1968.
- Mzhavia N, Berman Y, Che FY, Fricker LD, and Devi LA (2001) ProSAAS processing in mouse brain and pituitary. *J Biol Chem* **276**:6207–6213.
- Mzhavia N, Qian Y, Feng Y, Che FY, Devi LA, and Fricker LD (2002) Processing of proSAAS in neuroendocrine cell lines. *Biochem J* **361**:67–76.
- Parobchak N, Rao S, Negron A, Schaefer J, Bhattacharya M, Radovick S, and Babwah AV (2020) Uterine Gpr83 mRNA is highly expressed during early pregnancy and GPR83 mediates the actions of PEN in endometrial and non-endometrial cells. *F S Sci* **1**:67–77.
- Nguyen R, Venkatesan S, Binko M, Bang JY, Cajanding JD, Briggs C, Sargin D, Imayoshi I, Lambe EK, and Kim JC (2020) Cholecystokinin-Expressing Interneurons of the Medial Prefrontal Cortex Mediate Working Memory Retrieval. *J Neurosci* **40**:2314–2331.
- Okonkwo O, Zeffoff D, and Adeyinka A (2020) Biochemistry, Cholecystokinin, in *StatPearls*. StatPearls Publishing, Treasure Island, FL.
- Overduin J, Gibbs J, Cummings DE, and Reeve Jr JR (2014) CCK-58 elicits both satiety and satiation in rats while CCK-8 elicits only satiation. *Peptides* **54**:71–80.
- Pan H, Che FY, Peng B, Steiner DF, Pintar JE, and Fricker LD (2006) The role of prohormone convertase-2 in hypothalamic neuropeptide processing: a quantitative neuropeptidomic study. *J Neurochem* **98**:1763–1777.
- Pesini P, Dethoux M, Parmentier M, and Hökfelt T (1998) Distribution of a glucocorticoid-induced orphan receptor (JP05) mRNA in the central nervous system of the mouse. *Brain Res Mol Brain Res* **57**:281–300.
- Rehfeld JF (2017) Cholecystokinin-From Local Gut Hormone to Ubiquitous Messenger. *Front Endocrinol (Lausanne)* **8**:47.
- Rehfeld JF, Friis-Hansen L, Goetze JP, and Hansen TV (2007) The biology of cholecystokinin and gastrin peptides. *Curr Top Med Chem* **7**:1154–1165.
- Royds J, Conroy MJ, Dunne MR, Cassidy H, Matallanas D, Lysaght J, and McCrory C (2020) Examination and characterisation of burst spinal cord stimulation on cerebrospinal fluid cellular and protein constituents in patient responders with chronic neuropathic pain - A Pilot Study. *J Neuroimmunol* **344**:577249.
- Sah R, Parker SL, Sheriff S, Eaton K, Balasubramanian A, and Sallee FR (2007) Interaction of NPY compounds with the rat glucocorticoid-induced receptor (GIR) reveals similarity to the NPY-Y2 receptor. *Peptides* **28**:302–309.
- Sallee NA, Lee E, Leffert A, Ramirez S, Brace AD, Halenbeck R, Kavanaugh WM, and Sullivan KMC (2020) A Pilot Screen of a Novel Peptide Hormone Library Identified Candidate GPR83 Ligands. *SLAS Discov* **25**:1047–1063.
- Sayegh AI, Washington MC, Raboin SJ, Aglan AH, and Reeve Jr JR (2014) CCK-58 prolongs the intermeal interval, whereas CCK-8 reduces this interval: not all forms of cholecystokinin have equal bioactivity. *Peptides* **55**:120–125.
- Schiffmann SN and Vanderhaeghen JJ (1991) Distribution of cells containing mRNA encoding cholecystokinin in the rat central nervous system. *J Comp Neurol* **304**:219–233.
- Teixeira LB, Parreiras-E-Silva LT, Bruder-Nascimento T, Duarte DA, Simões SC, Costa RM, Rodriguez DY, Ferreira PAB, Silva CAA, Abrão EP et al. (2017) Ang-(1-7) is an endogenous β -arrestin-biased agonist of the AT₁ receptor with protective action in cardiac hypertrophy. *Sci Rep* **7**:11903.
- E Vollmer L, Ghosal S, A Rush J, R Sallee F, P Herman J, Weinert M, and Sah R (2013) Attenuated stress-evoked anxiety, increased sucrose preference and delayed spatial learning in glucocorticoid-induced receptor-deficient mice. *Genes Brain Behav* **12**:241–249.
- Wang D, Herman JP, Pritchard LM, Spitzer RH, Ahlbrand RL, Kramer GL, Petty F, Sallee FR, and Richtand NM (2001) Cloning, expression, and regulation of a glucocorticoid-induced receptor in rat brain: effect of repetitive amphetamine. *J Neurosci* **21**:9027–9035.
- Wardman JH, Berezniuk I, Di S, Tasker JG, and Fricker LD (2011) ProSAAS-derived peptides are colocalized with neuropeptide Y and function as neuropeptides in the regulation of food intake. *PLoS One* **6**:e28152.
- Wardman JH, Gomes I, Bobeck EN, Stockert JA, Kapoor A, Bisignano P, Gupta A, Mezei M, Kumar S, Filizola M, et al. (2016) Identification of a small-molecule ligand that activates the neuropeptide receptor GPR171 and increases food intake. *Sci Signal* **9**:ra55.
- Whissell PD, Cajanding JD, Fogel N, and Kim JC (2015) Comparative density of CCK- and PV-GABA cells within the cortex and hippocampus. *Front Neuroanat* **9**:124.
- You ZB, Herrera-Marschitz M, Brodin E, Meana JJ, Morino P, Hökfelt T, Silveira R, Gojny M, and Ungerstedt U (1994) On the origin of striatal cholecystokinin release: studies with in vivo microdialysis. *J Neurochem* **62**:76–85.
- Záborszky L, Alheid GF, Beinfeld MC, Eiden LE, Heimer L, and Palkovits M (1985) Cholecystokinin innervation of the ventral striatum: a morphological and radioimmunological study. *Neuroscience* **14**:427–453.
- Zhang X, Che FY, Berezniuk I, Sonmez K, Toll L, and Fricker LD (2008) Peptidomics of Cpe(fat/fat) mouse brain regions: implications for neuropeptide processing. *J Neurochem* **107**:1596–1613.
- Zhang X, Pan H, Peng B, Steiner DF, Pintar JE, and Fricker LD (2010) Neuropeptidomic analysis establishes a major role for prohormone convertase-2 in neuropeptide biosynthesis. *J Neurochem* **112**:1168–1179.

Address correspondence to: Lakshmi A. Devi, Department of Pharmacological Sciences, Icahn School of Medicine at Mount Sinai, 19-90 Annenberg Building, One Gustave L. Levy Place, New York, NY 10029. E-mail: Lakshmi.Devi@mssm.edu

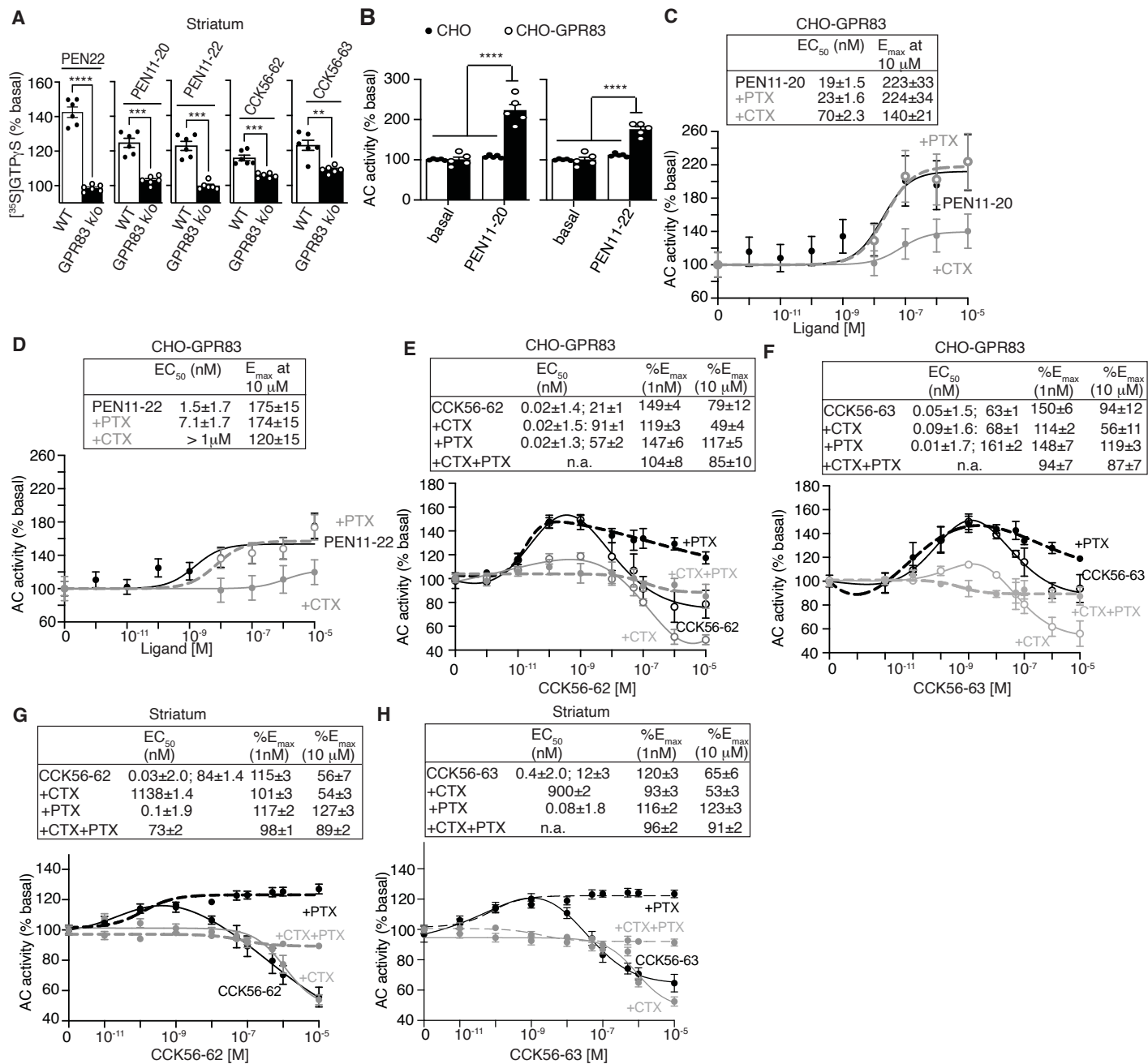
Supplemental Fig.1



Supplemental Fig. 1. Binding and signaling by C-terminally truncated PEN peptides.

(A) Displacement of [¹²⁵I]Tyr-rPEN binding by PEN22 to membranes (20 μg) from CHO cells alone (CHO) or from cells expressing GPR83 (CHO-GPR83). [¹²⁵I]Tyr-rPEN binding is seen in CHO-GPR83 but not in CHO membranes and is dose-dependently displaced by PEN22. Data represents Mean±SD (n=6). (B) C-terminally truncated PEN peptides increase [³⁵S]GTPγS binding to CHO-GPR83 but not CHO membranes (20 μg). Data represents Mean±SD (n=3). **p<0.01; ****p<0.0001 (Two-Way ANOVA with Tukey's multiple comparison tests). (C) C-terminally truncated PEN peptides modulate adenylyl cyclase (AC) activity in CHO-GPR83 but not CHO membranes (2 μg). Data represents Mean±SD (n=3). ****p<0.0001 (Two-Way ANOVA with Tukey's multiple comparison tests). (D-F) Modulation of adenylyl cyclase activity by C-terminally truncated PEN peptides in membranes (2 μg) from CHO-GPR83 cells. Signaling by PEN18 and PEN19 is blocked by CTX while that of PEN20 is blocked by PTX. Data represents Mean±SD (n=3). (G) C-terminally truncated PEN peptides increase phospholipase C activity in CHO-GPR83 but not CHO membranes (10 μg). Data represent mean±SD (n=6). ****p<0.0001 (Two-Way ANOVA with Tukey's multiple comparison tests). (H) C-terminally truncated PEN peptides increase intracellular calcium levels in CHO-GPR83 but not CHO cells. Data represents Mean±SD (n=3). **p<0.01; ***p<0.001; ****p<0.0001 (Two-Way ANOVA with Tukey's multiple comparison tests). (I) Displacement of [¹²⁵I]Tyr-rPEN binding by PEN22 to striatal membranes (20 μg) from wild-type (WT) or from GPR83 knockout (GPR83 KO) mice. [¹²⁵I]Tyr-rPEN binding is seen in WT but not in GPR83 KO membranes and is dose-dependently displaced by PEN22. Data represent Mean±SD (n=3). (J) C-terminally truncated PEN peptides increase phospholipase C activity in striatal membranes (10 μg) from WT but not GPR83 KO mice. Data represent Mean±SD (n=3). *p<0.05; **p<0.01; ***p<0.001 (unpaired t-test with Welch's correction).

Supplemental Fig. 2



Supplemental Fig.2. Signaling by proCCK-derived peptides and related PEN peptides.

(A) proCCK-derived peptides and related PEN peptide-mediated increases in [³⁵S]GTPγS binding to striatal membranes (20 μg) from wild-type (WT) and GPR83 knockout (GPR83 k/o) mice. Data represents Mean±SD (n=6). **p<0.01; ***p<0.001, ****p<0.0001; WT vs GPR83k/o; Unpaired t-test with Welch's correction). (B) PEN11-20 and PEN11-22 increase adenylyl cyclase (AC) activity in CHO-GPR83 but not CHO membranes (2 μg). Data represents Mean±SD (n=5). ****p<0.0001 (Two-Way ANOVA with Tukey's multiple comparison tests). (C-H) Modulation of adenylyl cyclase activity by proCCK-derived peptides (E-H) and related PEN peptides (C, D) in membranes (2 μg) from CHO-GPR83 (C-F) and striatum (G, H). A combination of CTX and PTX is needed to completely block signaling by pro-CCK-derived peptides (E-H) while related PEN peptide-mediated increase in adenylyl cyclase activity is blocked by CTX (C, D). Data represent mean±SEM (n=5 for C,D; n=4 for E-H).

GPR83 engages endogenous peptides from two distinct precursors to elicit differential signaling

Seshat M. Mack^{1a}, Ivone Gomes^{1a}, Amanda K. Fakira^{1,3}, Mariana L. Duarte¹, Achla Gupta¹, Lloyd Fricker², and Lakshmi A. Devi^{1*}
Molecular Pharmacology: MOLPHARM-AR-2022-000487

Supplemental Table 1. Displacement binding parameters by C-terminal truncated PEN peptides in membranes from CHO cells expressing GPR83 and from the striatum.

Ligand	Sequence	Membranes	% displaced at 10 μ M	IC ₅₀ [M]	n _H
PEN22	SVDQDLGPEVPPENVLGALLRV	CHO-GPR83	95 \pm 4	2.0 \pm 1.5E ⁻¹⁰ ; 1.1 \pm 1.5E ⁻⁶	42.73 \pm 1.1
PEN20	SVDQDLGPEVPPENVLGALL	CHO-GPR83	55 \pm 10	1.6 \pm 1.8E ⁻¹⁰ ; 2.9 \pm 4.6E ⁻⁶	55.35 \pm 1.27
PEN19	SVDQDLGPEVPPENVLGAL	CHO-GPR83	75 \pm 4	3.4 \pm 2.1E ⁻¹¹ ; 9.3 \pm 4.8E ⁻⁶	24.33 \pm 1.36
PEN18	SVDQDLGPEVPPENVLGA	CHO-GPR83	61 \pm 8	1.2 \pm 4.1E ⁻¹¹ ; 2.7 \pm 1.7E ⁻⁷	21.38 \pm 1.12
PEN22	SVDQDLGPEVPPENVLGALLRV	Striatum	99 \pm 1	1.8 \pm 1.5E ⁻¹⁰ ; 1.8 \pm 1.5E ⁻⁶	41.09 \pm 1.08
PEN20	SVDQDLGPEVPPENVLGALL	Striatum	61 \pm 3	2.0 \pm 2.3E ⁻¹⁰ ; 1.2 \pm 1.8E ⁻⁶	35.42 \pm 1.14
PEN19	SVDQDLGPEVPPENVLGAL	Striatum	72 \pm 3	5.0 \pm 1.8E ⁻¹¹ ; 3.1 \pm 2.1E ⁻⁶	38.12 \pm 1.13
PEN18	SVDQDLGPEVPPENVLGA	Striatum	56 \pm 4	6.4 \pm 4.4E ⁻¹¹ ; 2.6 \pm 1.7E ⁻⁷	22.09 \pm 1.15

Displacement binding assays were carried out with [¹²⁵I]Tyr-rPEN (3 nM) using membranes (20 μ g) from CHO cells stably expressing GPR83 (CHO-GPR83) or from the striatum in the absence or presence of different concentrations of PEN18, PEN19, PEN20 or PEN22 (10⁻¹⁵-10⁻⁵M) in 50 mM Tris-Cl buffer (pH 7.4) containing protease inhibitor cocktail as described in Methods. Data are Mean \pm SD (see Methods for details). n_H= % receptors in high affinity state.

GPR83 engages endogenous peptides from two distinct precursors to elicit differential signaling

Seshat M. Mack^{1a}, Ivone Gomes^{1a}, Amanda K. Fakira^{1,3}, Mariana L. Duarte¹, Achla Gupta¹, Lloyd Fricker², and Lakshmi A. Devi^{1*}

Molecular Pharmacology: MOLPHARM-AR-2022-000487

Supplemental Table 2. Signaling parameters by C-terminal truncated PEN peptides in membranes from CHO cells expressing GPR83 and from the striatum.

Ligand	Membranes	³⁵ S]GTPγS binding		Adenylyl cyclase activity		PLC activity		Intracellular Ca ²⁺ release		Receptor internalization			
		EC ₅₀ (nM)	%E _{max} at 10 μM	EC ₅₀ (nM)	% E _{max} at 10 μM	EC ₅₀ (nM)	% E _{max} at 10 μM	EC ₅₀ (nM)	% E _{max} at 10 μM	EC ₅₀ (nM)	% E _{max} at 10 μM	T _{1/2} (fast) (min)	T _{1/2} (slow) (min)
PEN18	CHO-GPR83	>1 μM	105±3	1.4±2.1	136±12	0.09±1.9	157±14	>1 μM	764±225	3.7±2.5	68±7	5.5±3.8	64±40
PEN19	CHO-GPR83	777±2	111±4	27±1.7	146±13	0.08±2.1	147±9	59±1.5	1002±264	0.9±2.4	49±6	3.3±3.8	37±53
PEN20	CHO-GPR83	0.8±2	118±3	11±2.9	72±9	2.5±1.8	199±43	0.04±3.3	632±262	2.7±1.4	49±4	2.2±2.2	77±55
PEN22	CHO-GPR83	0.9±2	126±3	10±2.1	66±7	3.2±1.6	315±44	8.8±1.4	1379±310	3.6±1.4	30±6	2.0±3.8	115±44
PEN18	Striatum	0.1±2.1	137±9	1.1±3.0	113±6	n.d.	117±18	-	-	-	-	-	-
PEN19	Striatum	<0.1 nM	120±8	>1 μM	117±6	n.d.	130±20	-	-	-	-	-	-
PEN20	Striatum	11±3.0	120±8	>1 μM	137±8	0.4±1.6	577±85	-	-	-	-	-	-
PEN22	Striatum	0.3±1.8	143±9	0.5±1.9	125±7	0.09±1.4	646±74	-	-	-	-	-	-

Membranes from CHO-GPR83 cells or from WT striatum were used for [³⁵S]GTPγS binding assay (20 μg), adenylyl cyclase activity assay (2 μg) or phospholipase C activity assay (10 μg). Assays were carried out as described in methods using C-terminally truncated PEN peptides (0-10 μM final concentration). CHO-GPR83 cells were used for measurement of intracellular Ca²⁺ release or receptor endocytosis (2 x 10⁵ cells/well) with C-terminally truncated PEN peptides (0-10 μM final concentration) as described in methods. For time course experiments cells were incubated with the peptides (100 nM) for 0-120 min. Data represent Mean±SD (see methods for details). - = not done.

GPR83 engages endogenous peptides from two distinct precursors to elicit differential signaling

Seshat M. Mack^{1a}, Ivone Gomes^{1a}, Amanda K. Fakira^{1,3}, Mariana L. Duarte¹, Achla Gupta¹, Lloyd Fricker², and Lakshmi A. Devi^{1*}
Molecular Pharmacology: MOLPHARM-AR-2022-000487

Supplemental Table 3. Displacement binding parameters by PEN11-20, PEN11-22 and related proCCK peptides in membranes from CHO cells expressing GPR83 and from the striatum.

Ligand	Sequence	Membranes	% displaced at 10 μ M	IC ₅₀ [M]	n _H
PEN22	SVDQDLGPEVPPENVLGALLRV	CHO-GPR83	95 \pm 4	2.0 \pm 1.5E ⁻¹⁰ ; 1.1 \pm 1.5E ⁻⁶	42.73 \pm 1.08
PEN11-20	PPENVLGALL	CHO-GPR83	73 \pm 7	8.1 \pm 1.3E ⁻¹² ; 2.1 \pm 1.4E ⁻⁷	47.90 \pm 1.06
PEN11-22	PPENVLGALLRV	CHO-GPR83	86 \pm 2	1.3 \pm 1.9E ⁻¹² ; 4.3 \pm 1.5E ⁻⁷	31.73 \pm 1.20
CCK56-62	ARLGALL	CHO-GPR83	54 \pm 3	4.6 \pm 1.8E ⁻¹¹ ; 1.5 \pm 1.8E ⁻⁷	46.02 \pm 1.12
CCK56-63	ARLGALLA	CHO-GPR83	44 \pm 4	4.2 \pm 2.1E ⁻¹⁰ ; 7.2 \pm 2.9E ⁻⁷	57.20 \pm 1.32
PEN22	SVDQDLGPEVPPENVLGALLRV	Striatum	99 \pm 1	1.6 \pm 1.4E ⁻¹⁰ ; 1.7 \pm 1.5E ⁻⁶	41.42 \pm 1.08
PEN11-20	PPENVLGALL	Striatum	64 \pm 10	6.9 \pm 3.3E ⁻¹² ; 1.3 \pm 2.0E ⁻⁷	58.59 \pm 1.12
PEN11-22	PPENVLGALLRV	Striatum	72 \pm 15	1.6 \pm 1.6E ⁻¹² ; 6.5 \pm 1.4E ⁻⁷	33.49 \pm 1.06
CCK56-62	ARLGALL	Striatum	52 \pm 2	5.7 \pm 1.5E ⁻¹² ; 9.0 \pm 1.4E ⁻⁸	42.92 \pm 1.08
CCK56-63	ARLGALLA	Striatum	39 \pm 3	4.1 \pm 1.9E ⁻¹¹ ; 3.8 \pm 1.6E ⁻⁸	38.85 \pm 1.14

Displacement binding assays were carried out with [¹²⁵I]Tyr-rPEN (3 nM) using membranes (20 μ g) from CHO cells stably expressing GPR83 (CHO-GPR83) or from WT striatum in the absence or presence of different concentrations of PEN11-20, PEN11-22, PEN22, CCK56-62 or CCK56-63 (10⁻¹⁵-10⁻⁵M) in 50 mM Tris-Cl buffer (pH 7.4) containing protease inhibitor cocktail as described in Methods. Data are Mean \pm SD (see methods for details). n_H= % receptors in high affinity state.

GPR83 engages endogenous peptides from two distinct precursors to elicit differential signaling

Seshat M. Mack^{1a}, Ivone Gomes^{1a}, Amanda K. Fakira^{1,3}, Mariana L. Duarte¹, Achla Gupta¹, Lloyd Fricker², and Lakshmi A. Devi^{1*}
Molecular Pharmacology: MOLPHARM-AR-2022-000487

Supplemental Table 4. Signaling parameters by PEN11-20, PEN11-22 in membranes from CHO cells expressing GPR83 and from the striatum.

Ligand	Membranes	³⁵ S]GTPγS binding		Adenylyl cyclase activity		Receptor internalization	
		EC ₅₀ (nM)	% E _{max} at 10 μM	EC ₅₀ (nM)	% E _{max} at 10 μM	EC ₅₀ (nM)	% E _{max} at 10 μM
PEN22	CHO-GPR83	0.9±2.0	126±3	10±2.1	66±7	3.6±1.4	30±6
PEN11-20	CHO-GPR83	-	-	19±1.5	223±33	1.1±1.6	48±2
PEN11-22	CHO-GPR83	-	-	1.5±1.7	175±15	0.6±1.6	35±5
CCK56-62	CHO-GPR83			0.01±1.3; 21±2.0	149±4*; 81±15	1.7±1.8	53±4
CCK56-63				0.05±1.5; 63±1.3	150±6*; 79±6	0.6±1.9	51±6
PEN22	Striatum	0.3±1.8	137±9	0.5±1.9	125±5	-	-
PEN11-20	Striatum	9.8±1.5	125±6	-	-	-	-
PEN11-22	Striatum	41±1.5	123±6	-	-	-	-
CCK56-62	Striatum	4.0±3.2	114±7	0.03±2.0; 84±1.4	115±3*; 56±6	-	-
CCK56-63	Striatum	33±1.7	130±7	0.4±2; 12±3	120±3*; 65±6	-	-

Membranes (20 μg) from WT striatum were subjected to a [³⁵S]GTPγS binding assay with proCCK-derived peptides and related PEN peptides (0-10 μM final concentration) as described in Methods. Membranes (2 μg) from CHO-GPR83 or WT striatum were probed for adenylyl cyclase activity with proCCK-derived peptides and related PEN peptides (0-10 μM final concentration) as described in Methods. Internalization of GPR83 by proCCK-derived peptides and related PEN peptides (0-10 μM final concentration) was measured in CHO-GPR83 cells (2 x 10⁵ cells/well) as described in methods. Data represent mean±SD (see details for n in methods). - = not done; *% E_{max} at 1 nM.